JACS
JOURNAL OF THE AMERICAN CHEMICAL SOCIETY
Communication
pubs.acs.org/JACS

Controlling the Metal to Semiconductor Transition of MoS_2 and WS_2 in Solution

Stanley S. Chou,*[,†] Yi-Kai Huang,[‡] Jaemyung Kim,[‡] Bryan Kaehr,[†] Brian M. Foley,[§] Ping Lu,[†] Conner Dykstra,[‡,∥] Patrick E. Hopkins,[§] C. Jeffrey Brinker,[†,∥] Jiaxing Huang,*[,‡] and Vinayak P. Dravid*[,‡]

[†]Advanced Materials Laboratory, Sandia National Laboratories, Albuquerque, New Mexico 87185, United States

[‡]Department of Materials Science and Engineering, International Institute of Nanotechnology, Northwestern University, Evanston, Illinois 60208, United States

[§]Department of Mechanical and Aerospace Engineering, University of Virginia, Charlottesville, Virginia 22904, United States

[∥]Department of Chemical and Biomolecular Engineering, Center for Micro-engineered Materials, University of New Mexico, Albuquerque, New Mexico 87106, United States

Supporting Information

ABSTRACT: Lithiation-exfoliation produces single to few-layered MoS_2 and WS_2 sheets dispersible in water. However, the process transforms them from the pristine semiconducting 2H phase to a distorted metallic phase. Recovery of the semiconducting properties typically involves heating of the chemically exfoliated sheets at elevated temperatures. Therefore, it has been largely limited to sheets deposited on solid substrates. Here, we report the dispersion of chemically exfoliated MoS_2 sheets in high boiling point organic solvents enabled by surface functionalization and the controllable recovery of their semiconducting properties directly in solution. This process connects the scalability of chemical exfoliation with the simplicity of solution processing, ultimately enabling a facile method for tuning the metal to semiconductor transitions of MoS_2 and WS_2 within a liquid medium.

Molybdenum disulfide (MoS_2) and tungsten disulfide (WS_2) are part of an extended transition metal dichalcogenides family (MX_2) of inorganic solids composed of two-dimensional (2D) layers held together by weak intermolecular forces. Similar to graphite, monolayers can be exfoliated chemically[1,2] or mechanically,[3,4] yielding materials with optical, electronic, and chemical properties divergent from their bulk counterparts.[5−10]

Of the aforementioned methods, the chemical exfoliation method is notable because of its simplicity and scalability, with each reaction capable of yielding liters of dispersed mono and few layer sheets.[2,11,12] This process operates by intercalating MoS_2 and WS_2 with lithium to weaken interlayer attraction, and then dispersing single to few layered sheets into water with assistance of ultrasonication.[2,13]

Accompanying chemical exfoliation, however, is the introduction of a metallic phase, making the composition of the resultant sheets varied.[14] At present, tuning the phase composition of these sheets, from metal to semiconductor, is limited to drying from liquid onto heat-tolerant substrates, followed by annealing at elevated temperatures (ca. 300 °C).[15,16]

However, because drying from solution limits the processability of the exfoliated materials, there is thus desire to control the phase composition of the sheets directly in solution. In doing so, it would enable broader applicability for scalable processing and device integration.

To accomplish this, it would be ideal to anneal sheets in inert, high boiling point organic solvents that can withstand elevated temperatures without degrading the exfoliated sheets, such as octadecene or *o*-dichlorobenzene (ODCB). However, this is hindered by the poor dispersibility of chemically exfoliated sheets in organic solvents due to their highly negatively charged surface.[17] Moreover, since annealing restores the hydrophobic semiconducting phase,[18] annealing in polar solvents induces flocculation. Furthermore, as exfoliated monolayers are prone to oxidation, heating in even partially oxygenated environments, such as in most polar solvents, can quickly degrade the material.[19]

To solve this problem, we present a one-step surface functionalization of chemically exfoliated MoS_2 to enable their transfer from water to diverse classes of inert organic solvents. Heating the sheets in inert, high boiling point solvents makes it possible to tune their phase compositions and control the metal-to-semiconductor transition with minimal risk of oxygenation. Moreover, the resultant sheets maintain their solution processability and can be assembled into pliable and transferable free-standing films. Our method is potentially extendable to other MX_2 materials of interest, such as WS_2. Dispersity in organic solvents and in situ property tuning should significantly broaden the capability of solution processing of these two-dimensional sheets for potential device applications.

To exfoliate MoS_2 with Li intercalation into water, we followed previously described methods with slight modifications (Supporting Information).[17,20,21] The chemically exfoliated sheets were then transferred from water into inert nonpolar solvent via a biphasic reaction by using a weakly cationic amphiphile, oleylamine, dissolved in excess in the nonpolar solvent. The oleylamine's nitrogen terminus allows for electrostatic binding to the sheets. Upon sufficient coverage, the ligand forms a hydrophobic coating, which enables phase transfer

Received: October 18, 2014
Published: January 22, 2015

DOI: 10.1021/ja5107145
J. Am. Chem. Soc. 2015, 137, 1742−1745

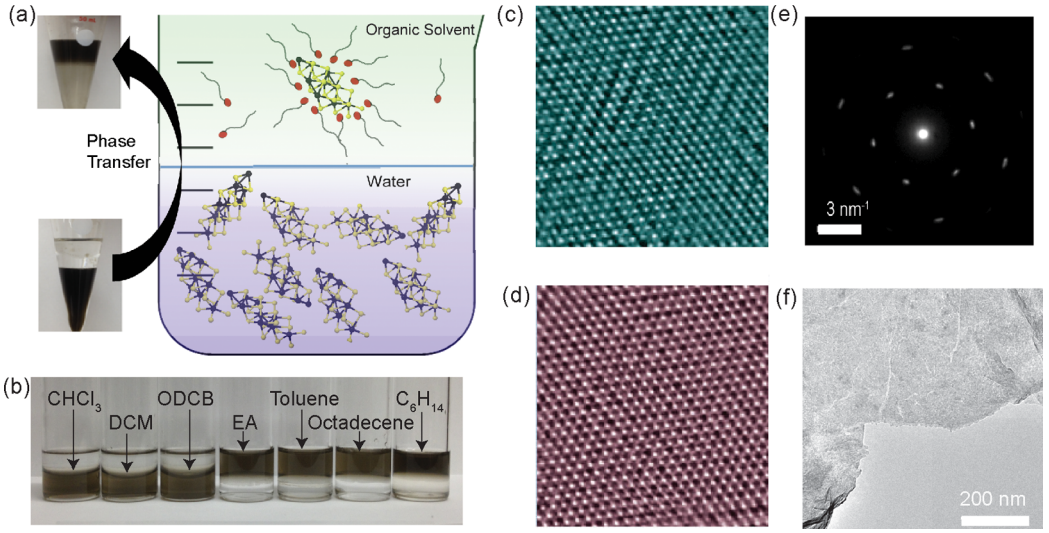

Figure 1. (a) Phase transfer of chemically exfoliated MoS_2 from water into inert high boiling point, organic solvents. (b) MoS_2 in organic solvents with decreasing polarity, from chloroform ($CHCl_3$), dichloromethane (DCM), ODCB, ethyl acetate (EA), and toluene to octadecene and hexane (C_6H_{14}). Colorless portion is water. (c) High-resolution STEM of MoS_2 after exfoliation. (d) STEM of MoS_2 after annealing. Images were false colored for clarity. (e) Diffraction pattern after annealing. (f) Morphology of MoS_2 sheets after annealing.

(Figure 1a). As seen in Figure 1b, this process transfers and disperses chemically exfoliated MoS_2 into most nonpolar organic solvents. For the purpose of annealing, inert high boiling point solvents such as ODCB (bp 180 °C) and octadecene (bp 315 °C) were most useful. For most transfers, the MoS_2 concentration plateaus at 0.5 mg/mL within the organic solvent. On the basis of thermogravimetric analysis, the binding ratio of MoS_2 to ligand is 1:3; the remainder of ligands is kept in solution as excess (Figure S1). Care should be taken at this point to thoroughly purge the air with N_2 or Ar. Following the purge, solutions were heated to near reflux for 4 h. The annealed samples were then collected with centrifugation and redispersed in hexane containing 2.5% oleylamine. As seen in Figure 1c, before annealing, Mo atoms on the basal plane exhibited patches of clustered Mo, with short (2.8 ± 0.3 Å) and long (3.8 ± 0.3 Å) periodicities in Mo−Mo distance. This in turn gives rise to zigzag-like patterns and a superlattice formation.[22,23] In the literature, this phase is alternatively dubbed the 1T′ or 1T and is a p-type conductor.[14,16,24−29] After annealing in octadecene (300 °C), the superlattice disappears, and a typical Mo lattice spacing of 3.15 Å can be seen (Figure 1d,e). This is indicative of the metal to semiconductor transition to the 2H phase.[30] It should be noted that after annealing the material maintains a sheet-like morphology (Figure 1f).

Previously, a correlation between X-ray photoelectron spectra (XPS) and the metal to semiconductor transition was shown, using the changing bonding states of Mo and S.[15] We similarly corroborate TEM results showing the phase transition with XPS, following annealing at different solution temperatures (Figure 2a). For this analysis, we calibrated our system using the carbon sp^2 C−C peak (284.6 eV) and then measured 2H peak positions using a single crystal MoS_2 reference. These resulting reference spectra, with Mo $3d^{5/2}$ at 229.1 eV and its doublet, Mo $3d^{3/2}$, at 3.15 eV higher, then served as references for the 2H in the remaining samples. Peak positions for the 1T′ phase was obtained using freshly exfoliated samples, which showed additional, non-2H peaks at 228.1 eV (1T′ Mo $3d^{5/2}$) and 231.3 eV (1T′ Mo $3d^{3/2}$).[15,31] Phase percentages were then calculated by peak area ratios of Mo $3d^{5/2}$ (Mo $3d^{3/2}$ peak heights

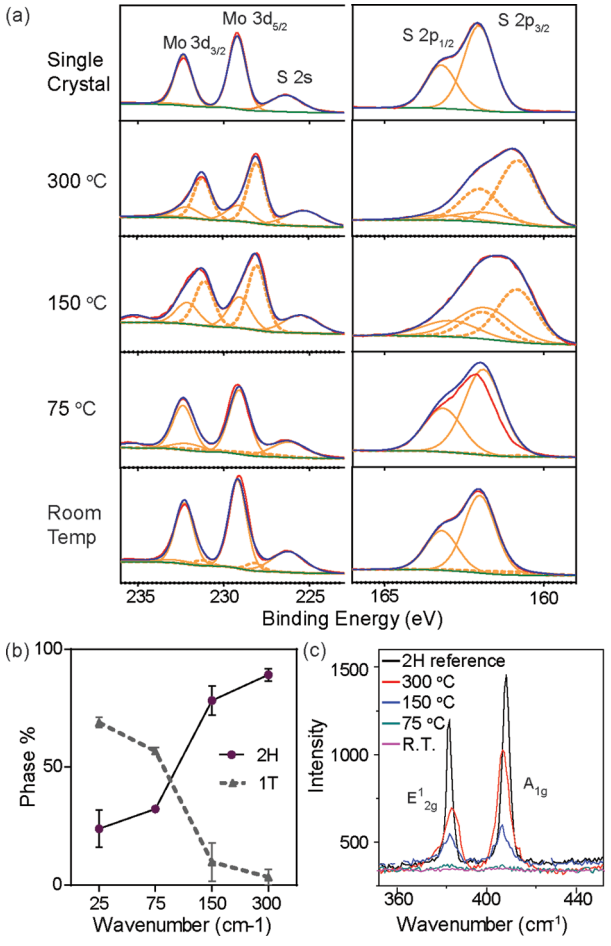

Figure 2. (a) XPS spectra of MoS_2 annealed at increasing solution temperatures, for 4 h each. (b) Corresponding phase percentage from XPS spectra and (c) Raman spectra.

were constrained based on $3d^{5/2}$ and thus not used in analysis). The same analysis was extended to the complementary sulfur spectra, with S 2H $2p^{3/2}$ peak at 161.9 eV and 1T′ $2p^{3/2}$ peak at

DOI: 10.1021/ja5107145
J. Am. Chem. Soc. 2015, 137, 1742−1745

160.9 eV, yielding corroborating results (for a detailed fitting procedure and summary, please see Tables S1 and S2).

A summary of this analysis can be seen in Figure 2b, with peak fittings for the metallic 1T′ being most prominent in freshly exfoliated, room temperature samples (69.0 ± 2.1%). With increasing solution temperature, 1T′ percentages began to decrease, and 2H percentage began to increase. First, after heating to 75 °C, the 2H phase fraction was raised from 23.9 ± 7.8% to 32.3 ± 0.6%. Further, at a 150 °C, 2H fractions reached 78.3 ± 6.2%, and at 300 °C, the 2H phase was 89.2 ± 2.7%. As shown in Figure 2b, the major metal to semiconductor (1T′ → 2H) transitions occurred between 75 and 150 °C, which is within the range of literature reports.[15,22,27]

Nonetheless, high temperature processing has a tendency to oxidize MoS_2.[19] For example, Mo spectra of MoS_2 annealed in ethylene glycols will produce prominent oxidation peaks at 235 to 236 eV (Figure S2). However, spectra in Figure 2a showed minimal oxidative peaks indicating the inert organic solvents were effective in averting oxidative degradation. This is confirmed with an analysis of the oxidative peaks in the Mo spectra, which show minimal difference between processed samples and controls (Table S3).

The phase transition was further corroborated using Raman spectroscopy. Previously, it was reported that with chemical exfoliation, 2H Raman signatures are attenuated.[32,33] Correspondingly, we observed restoration of 2H signatures with increasing solution temperature (Figure 2c). In particular, E^1_{2g} at 383.2 cm^{-1} and A^1_g at 405.1 cm^{-1} become increasingly prominent with solution annealing. This corroborates the TEM and XPS results for the metal to semiconductor transition. Further, we observe that the ratio of E^1_{2g}, in-plane vibration mode to A^1_g, the out of plane vibration mode, were maintained near 0.8. As the ratio is an indicator of grains size distribution, 0.8 indicates small, submicron grain sizes.[17] This is not surprising, as chemically exfoliated sheets are typically submicron. Further, the result is comparable to the synthetic precursors used here, and those seen on some CVD grown MoS_2 films.[34]

To assemble free-standing films for device measurements, MoS_2 solution was filtered over aluminum oxide membranes. In general, we found that films were easily transferable to arbitrary substrates (Figure 3a). Similar to individual sheets (Figure S3), the assembled MoS_2 films displayed increased photoluminescence in correspondence to raised solution annealing temperature (Figure 3b). It is likely that films with a predominance of the metallic 1T′ induce photoquenching within the specimen.[35] As samples were annealed, the metallic 1T′ phase transitioned to the semiconducting 2H phase, thus reducing propensity for quenching and giving rise to increased photoluminescence. Corresponding to the photoluminescence measurements, four-probe measurements of films yielded corroborative evidence of a conductor to semiconductor transition in relation to increased 2H fractions. On the whole, the resistance undergoes a 5 order of magnitude transition in correspondence to the solution heating temperature (Figure 3e). Furthermore, resistance scaled in proportion to 2H fractions (Figure 3f). To cross validate the metal−semiconductor transition, a 300 °C film was configured as a transistor using a polyelectrolyte gate (Figure S4). Here, the film exhibited p-type conductivity, which is consistent with previous reports using the chemical exfoliation process.[27] Additionally, an I_{on}/I_{off} ratio was observed with the annealed specimens. Comparatively, the predominantly 1T samples show no gate modulation, due to their conductive behavior.

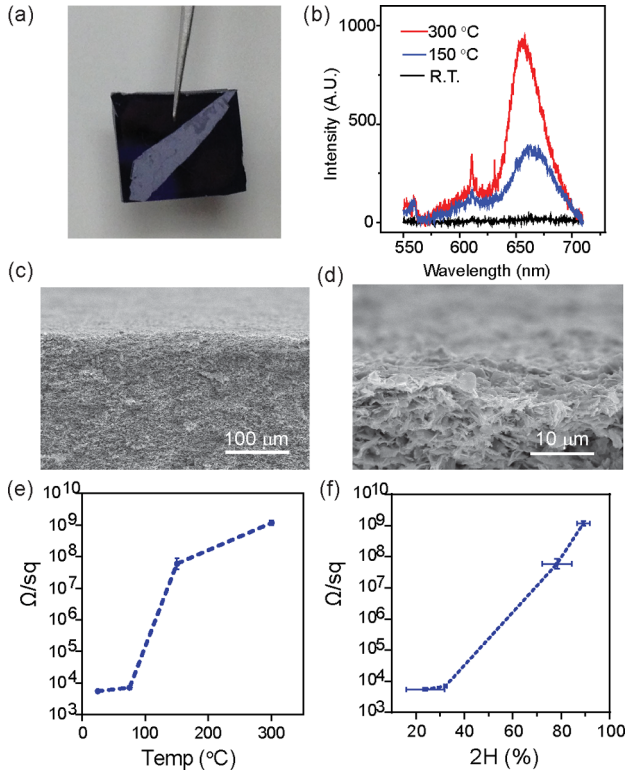

Figure 3. (a) MoS_2 film transferred onto secondary substrate. (b) Photoluminescence evolution with solution temperature. (c,d) Cross-sectional profile of free-standing MoS_2 film. (e) Sheet resistance of films processed at different solution temperatures. (f) Sheet resistance as a function of 2H.

Analogous experiments with chemically exfoliated WS_2 yielded results similar to MoS_2. As shown in Figure S5, the functionalization process transferred chemically exfoliated WS_2 sheets from water into organic solvents. Further, XPS signatures from chemical exfoliation were removed after annealing in liquid. This again demonstrates an effective metal to semiconductor conversion in solution. As the ligand attachment process is governed by electrostatic charge, we suspect this method may be adopted toward other 2D materials that contain anionic charges on the basal plane, including MX_2 materials that can be exfoliated with the assistance of Li intercalation.

In summary, we have described the transference of chemically exfoliated MX_2 sheets from water into nonpolar organic solvents through surface functionalization, thus overcoming the incompatibility of chemically exfoliated sheets with inert organic solvents. Furthermore, by selecting inert organic solvents with appropriate boiling point, we can thermally anneal the sheets in liquid to enable a metal to semiconductor transition with minimal oxidative degradation. These can be assembled into macroscopic free-standing films and patterns and can be transferred onto secondary substrates or used as unsupported papers. This process synergistically integrates the scalability of chemical exfoliation with ease of solution processing, thereby enabling a facile method for tuning their metal to semiconductor transition in solution.

DOI: 10.1021/ja5107145
J. Am. Chem. Soc. 2015, 137, 1742−1745

■ ASSOCIATED CONTENT

Supporting Information

Experimental procedures and additional characterization data. This material is available free of charge via the Internet at http://pubs.acs.org.

■ AUTHOR INFORMATION

Corresponding Authors

*v-dravid@northwestern.edu.
*jiaxing-huang@northwestern.edu.
*schou@sandia.gov.

Notes

The authors declare no competing financial interest.

■ ACKNOWLEDGMENTS

S.C., B.K., and C.J.B. acknowledge the U.S. Department of Energy, Office of Science, Basic Energy Sciences, Materials Sciences and Engineering Division for support. J.H. thanks the NSF for a CAREER Award (DMR 0955612). V.P.D. acknowledges support by the National Cancer Institute Center for Cancer Nanotechnology Excellence (CCNE) initiative at Northwestern University award number U54A119341. B.M.F. and P.E.H. are appreciative for funding from the Army Research Office (W911NF-13-4-0528). Sandia National Laboratories is managed and operated by Sandia Corporation, a wholly owned subsidiary of Lockheed Martin Corporation, for the U.S. Department of Energy's National Nuclear Security Administration under contract number DE-AC04-94AL85000. Parts of this work made use of the NUANCE facility with support from NSF-NSEC, NSF-MRSEC, the Keck Foundation, the State of Illinois, and Northwestern University. We thank Dr. M. Lilly and Dr. T. Harris for assistance with four probe measurements at the Center for Integrated Nanotechnologies, an Office of Science User Facility operated for the U.S. Department of Energy Office of Science by Los Alamos National Laboratory and Sandia National Laboratories.

■ REFERENCES

(1) Divigalpitiya, W. M. R.; Frindt, R. F.; Morrison, S. R. *Science* **1989**, *246*, 369.
(2) Joensen, P.; Frindt, R. F.; Morrison, S. R. *Mater. Res. Bull.* **1986**, *21*, 457.
(3) Li, H.; Wu, J.; Yin, Z.; Zhang, H. *Acc. Chem. Res.* **2014**, *47*, 1067.
(4) Radisavljevic, B.; Radenovic, A.; Brivio, J.; Giacometti, V.; Kis, A. *Nat. Nano* **2011**, *6*, 147.
(5) Late, D. J.; Liu, B.; Matte, H. S. S. R.; Rao, C. N. R.; Dravid, V. P. *Adv. Funct. Mater.* **2012**, *22*, 1894.
(6) Li, H.; Lu, G.; Yin, Z.; He, Q.; Li, H.; Zhang, Q.; Zhang, H. *Small* **2012**, *8*, 682.
(7) Huang, X.; Tan, C.; Yin, Z.; Zhang, H. *Adv. Mater.* **2014**, *26*, 2185.
(8) Huang, X.; Zeng, Z.; Zhang, H. *Chem. Soc. Rev.* **2013**, *42*, 1934.
(9) Butler, S. Z.; Hollen, S. M.; Cao, L.; Cui, Y.; Gupta, J. A.; Gutiérrez, H. R.; Heinz, T. F.; Hong, S. S.; Huang, J.; Ismach, A. F.; Johnston-Halperin, E.; Kuno, M.; Plashnitsa, V. V.; Robinson, R. D.; Ruoff, R. S.; Salahuddin, S.; Shan, J.; Shi, L.; Spencer, M. G.; Terrones, M.; Windl, W.; Goldberger, J. E. *ACS Nano* **2013**, *7*, 2898.
(10) Wang, Q. H.; Kalantar-Zadeh, K.; Kis, A.; Coleman, J. N.; Strano, M. S. *Nat. Nano* **2012**, *7*, 699.
(11) Zeng, Z.; Yin, Z.; Huang, X.; Li, H.; He, Q.; Lu, G.; Boey, F.; Zhang, H. *Angew. Chem., Int. Ed.* **2011**, *50*, 11093.
(12) Zeng, Z.; Sun, T.; Zhu, J.; Huang, X.; Yin, Z.; Lu, G.; Fan, Z.; Yan, Q.; Hng, H. H.; Zhang, H. *Angew. Chem., Int. Ed.* **2012**, *51*, 9052.
(13) Miremadi, B. K.; Morrison, S. R. *J. Appl. Phys.* **1988**, *63*, 4970.
(14) Wypych, F.; Schollhorn, R. *J. Chem. Soc., Chem. Commun.* **1992**, 1386.
(15) Eda, G.; Yamaguchi, H.; Voiry, D.; Fujita, T.; Chen, M.; Chhowalla, M. *Nano Lett.* **2011**, *11*, 5111.
(16) Voiry, D.; Yamaguchi, H.; Li, J.; Silva, R.; Alves, D. C. B.; Fujita, T.; Chen, M.; Asefa, T.; Shenoy, V. B.; Eda, G.; Chhowalla, M. *Nat. Mater.* **2013**, *12*, 850.
(17) Chou, S. S.; Kaehr, B.; Kim, J.; Foley, B. M.; De, M.; Hopkins, P. E.; Huang, J.; Brinker, C. J.; Dravid, V. P. *Angew. Chem., Int. Ed.* **2013**, *52*, 4160.
(18) Ozcan, O. *Int. J. Miner. Process.* **1992**, *34*, 191.
(19) Windom, B.; Sawyer, W. G.; Hahn, D. *Tribol. Lett.* **2011**, *42*, 301.
(20) Chou, S. S.; De, M.; Kim, J.; Byun, S.; Dykstra, C.; Yu, J.; Huang, J.; Dravid, V. P. *J. Am. Chem. Soc.* **2013**, *135*, 4584.
(21) Kim, J.; Byun, S.; Smith, A. J.; Yu, J.; Huang, J. *J. Phys. Chem. Lett.* **2013**, *4*, 1227.
(22) Dungey, K. E.; Curtis, M. D.; Penner-Hahn, J. E. *Chem. Mater.* **1998**, *10*, 2152.
(23) Petkov, V.; Billinge, S. J. L.; Larson, P.; Mahanti, S. D.; Vogt, T.; Rangan, K. K.; Kanatzidis, M. G. *Phys. Rev. B* **2002**, *65*, 092105.
(24) Chen, X.; Chen, Z.; Li, J. *Chin. Sci. Bull.* **2013**, *58*, 1632.
(25) Kan, M.; Wang, J. Y.; Li, X. W.; Zhang, S. H.; Li, Y. W.; Kawazoe, Y.; Sun, Q.; Jena, P. *J. Phys. Chem. C* **2014**, *118*, 1515.
(26) Eda, G.; Fujita, T.; Yamaguchi, H.; Voiry, D.; Chen, M.; Chhowalla, M. *ACS Nano* **2012**, *6*, 7311.
(27) Heising, J.; Kanatzidis, M. G. *J. Am. Chem. Soc.* **1999**, *121*, 11720.
(28) Py, M. A.; Haering, R. R. *Can. J. Phys.* **1983**, *61*, 76.
(29) Voiry, D.; Salehi, M.; Silva, R.; Fujita, T.; Chen, M.; Asefa, T.; Shenoy, V. B.; Eda, G.; Chhowalla, M. *Nano Lett.* **2013**, *13*, 6222.
(30) Joensen, P.; Crozier, E. D.; Alberding, N.; Frindt, R. F. *J. Phys. C* **1987**, *20*, 4043.
(31) Papageorgopoulos, C. A.; Jaegermann, W. *Surf. Sci.* **1995**, *338*, 83.
(32) Yang, D.; Sandoval, S. J.; Divigalpitiya, W. M. R.; Irwin, J. C.; Frindt, R. F. *Phys. Rev. B* **1991**, *43*, 12053.
(33) Sekine, T.; Julien, C.; Samaras, I.; Jouanne, M.; Balkanski, M. *Mater. Sci. Eng., B* **1989**, *3*, 153.
(34) Zhan, Y.; Liu, Z.; Najmaei, S.; Ajayan, P. M.; Lou, J. *Small* **2012**, *8*, 966.
(35) Tan, A. T. L.; Kim, J.; Huang, J.-K.; Li, L.-J.; Huang, J. *Small* **2013**, *9*, 3252.

DOI: 10.1021/ja5107145
J. Am. Chem. Soc. 2015, 137, 1742−1745